

## Strongly Coupled Optical Phonons in the Ultrafast Dynamics of the Electronic Energy and Current Relaxation in Graphite

Tobias Kampfrath, Luca Perfetti, Florian Schapper, Christian Frischkorn, and Martin Wolf

*Fachbereich Physik, Freie Universität Berlin, Arnimallee 14, 14195 Berlin, Germany*

(Received 22 February 2005; published 26 October 2005)

Ultrafast charge carrier dynamics in graphite has been investigated by time-resolved terahertz spectroscopy. Analysis of the transient dielectric function and model calculations show that more than 90% of the initially deposited excitation energy is transferred to a few strongly coupled lattice vibrations within 500 fs. These hot optical phonons also substantially contribute to the striking increase of the Drude relaxation rate observed during the first picosecond after photoexcitation. The subsequent cooling of the hot phonons yields a lifetime estimate of 7 ps for these modes.

DOI: [10.1103/PhysRevLett.95.187403](https://doi.org/10.1103/PhysRevLett.95.187403)

PACS numbers: 78.47.+p, 71.38.-k, 72.80.-r, 81.05.Uw

Graphite has attracted continuous attention in research over the past decades [1]. Recently, a strong ambipolar electric field effect was found in thin films of this semimetal, thereby demonstrating its potential for future electronics [2]. Moreover, graphite is closely related to carbon nanotubes, which are the focus of nanotechnology research [3]. The latest experimental and theoretical efforts revealed that optical phonons in graphite strongly interact with the electrons [4,5]. These strongly coupled optical phonons (SCOPs) have high quantum energies of up to 0.2 eV and can be excited only by electrons of elevated energy. The scattering of electrons by SCOPs is believed to increase the dc resistivity of carbon nanotubes when high electric fields are applied [3]. In view of possible applications in electronics, further investigations are required on how SCOPs influence the transport and energy relaxation of electrons. Time-resolved terahertz spectroscopy (TRTS) is a promising experimental approach to this question. A visible pump pulse excites charge carriers in the sample and thus enables them to generate optical phonons. A subsequent terahertz (THz) pulse probes the low-energy response of the system ( $2\pi\hbar \times 1 \text{ THz} = 4.1 \text{ meV}$ ) such as the transport relaxation of charge carriers. The same technique has been successfully employed to study the dynamics of charge carriers in, for example, semiconductors [6] and superconductors [7].

In this Letter, we report on the application of TRTS to the semimetal graphite and present time-resolved measurements of its complex dielectric function after ultrafast optical excitation. Use of appropriate theoretical models enables us to extract the temporal evolution of three important observables of the excited system: the electronic temperature  $T_e$ , the plasma frequency  $\omega_{\text{pl}}$ , and the Drude relaxation rate  $\gamma$ . The latter quantifies the decay of an electronic current when the driving electric field is switched off. Our TRTS data exhibit a twofold relaxation dynamics after photoexcitation. Within the first 500 fs, the excited electrons thermalize and lose more than 90% of their initial excess energy. The small Fermi surface of graphite and wave vector conservation imply that the elec-

tronic energy is transferred to only a few phonon modes. Our simulations based on the two-temperature model [8] and latest calculations of electron-phonon (*e-ph*) coupling in graphite [5] reveal that this ultrafast electronic energy relaxation is dominated by the generation of hot optical phonons. The slower component of the observed relaxation dynamics is attributed to the cooling of the hot SCOPs. We obtain a lifetime estimate of 7 ps for these phonon modes. To the best of our knowledge, the occurrence of hot phonons in an optically excited semimetal is outlined here for the first time. In addition, the Drude relaxation rate is found to increase by more than 30% during the first picosecond after excitation. This effect is at least one order of magnitude larger than observed in comparable experiments on doped semiconductors [9]. Our numerical estimates using second-order perturbation theory [10,11] show that scattering of electrons by SCOPs is consistent with the observed rise of  $\gamma$ .

Our experimental setup employs a Ti:sapphire oscillator which delivers 10 fs laser pulses at 780 nm center wavelength, where 40% of the output is used to excite the sample. 100 fs THz pulses covering a spectral range from 8 to 30 THz are generated by difference frequency mixing in a GaSe crystal [12]. The THz electric field is detected by electro-optic sampling in ZnTe [13]. Graphite films are obtained by peeling off flakes from a high quality crystal of highly oriented pyrolytic graphite. We use a film of only 17 nm thickness, which guarantees a homogeneously excited probe volume. The polarization of the THz pulses is perpendicular to the graphite *c* axis, thus probing the optical properties in the basal plane. Our setup allows us to simultaneously measure both THz electric fields  $E_0(t)$  and  $E_0(t) + \Delta E_r(t)$  transmitted through the unexcited and excited sample, respectively. Here  $t$  denotes the local time of the THz pulse and  $\tau$  the delay between pump and probe pulse. The dielectric function  $\epsilon_0(\omega)$  of the unexcited sample is determined from transmission measurements covering frequencies  $\omega/2\pi$  from 10 to 26 THz and 1 to 3 THz. All measurements are performed at room temperature in air.

Figure 1(a) shows  $E_0(t)$  and  $\Delta E_\tau(t)$  for an exemplary delay of  $\tau = 0.5$  ps. When the THz signal is sampled at a fixed value of the local time  $t$ , one obtains the pump-induced change  $\Delta E_\tau(t)$  as a function of the pump-probe delay  $\tau$  as plotted in Fig. 1(b) for  $t = -12$  fs. This trace exhibits a biexponential decay with time constants of 0.4 and 4 ps, respectively. However, much more information is gained from our TRTS data when we follow a quasistatic approach to determine the complex dielectric function  $\varepsilon_0(\omega) + \Delta\varepsilon_\tau(\omega)$  of graphite at time  $\tau$  after optical excitation [14].

Figure 1(c) displays the pump-induced changes of the dielectric function at  $\tau = 0.5$  ps. Its imaginary part features an interesting spectral behavior: For lower frequencies,  $\text{Im}\varepsilon$  and, thus, the THz absorption increase, whereas for frequencies above 15 THz a decrease of absorption (“bleaching”) is found. This effect can be explained by means of the simplified graphite band structure sketched in Fig. 2: A Bloch electron can either absorb a probing THz photon by a *direct* optical transition (DOT), which conserves the electron wave vector  $\mathbf{k}$ , or by an *indirect* optical transition (IOT), which requires some additional wave vector  $\Delta\mathbf{k}$ . The latter can be provided by scattering with phonons, lattice defects, or other electrons. Exciting the sample with a pump pulse transfers electrons from the valence band to the conduction band. After  $\approx 0.5$  ps, these hot electrons have thermalized and can be described by a

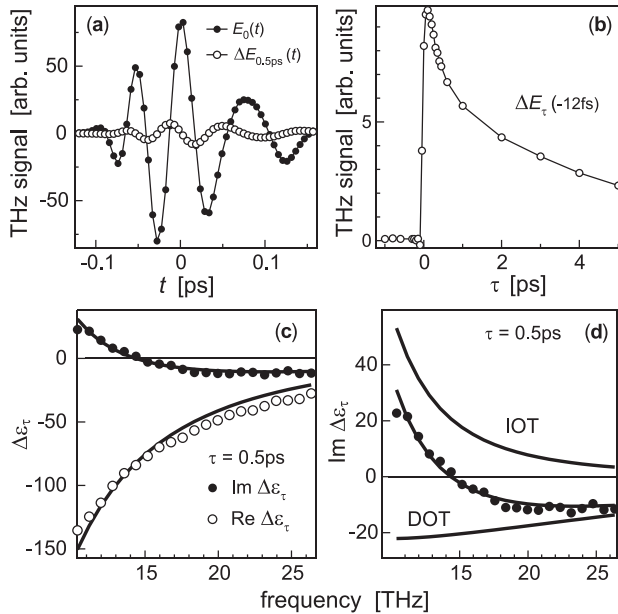


FIG. 1. (a) THz waveform  $E_0(t)$  transmitted through unexcited graphite and the pump-induced changes  $\Delta E_\tau(t)$  at  $\tau = 0.5$  ps. (b) Change in the THz electric field at  $t = -12$  fs as a function of the pump-probe delay  $\tau$ . (c) Pump-induced changes  $\Delta\varepsilon_\tau$  of the in-plane dielectric function of graphite at  $\tau = 0.5$  ps after photoexcitation. Thick solid lines are model fits (see text). (d) Magnified section of the imaginary part of  $\Delta\varepsilon_{0.5\text{ps}}$  with model fit and respective contributions of direct and indirect optical transitions.

Fermi-Dirac distribution with electronic temperature  $T_e$  as found by time-resolved photoemission spectroscopy (TRPES) [15]. The newly created electron-hole pairs block some of the originally possible DOTs in a range of  $k_B T_e$  around the Fermi energy  $E_F$  and decrease the absorption of photons  $\hbar\omega \sim k_B T_e$ . However, the elevated electronic temperature enables additional IOTs, thus leading to an increased THz absorption. Therefore, the frequency dependence of  $\text{Im}\Delta\varepsilon_\tau$  displayed in Fig. 1(c) reflects the interplay between DOTs and IOTs in graphite. In contrast, the graphite response to probe pulses in the visible is mediated mainly by DOTs [16].

For further analysis, we assume a thermalized electron gas and fit our measured  $\Delta\varepsilon_\tau$  to a model dielectric function  $\Delta\varepsilon^{\text{IOT}}(\omega_{\text{pl}}, \gamma) + \Delta\varepsilon^{\text{DOT}}(T_e)$  with fit parameters  $\omega_{\text{pl}}$ ,  $\gamma$ , and  $T_e$ . We employ the Drude formula  $\varepsilon^{\text{IOT}} = -\omega_{\text{pl}}^2/(\omega^2 + i\gamma\omega)$  for IOTs [17] and linear response formalism for DOTs [18,19]. The latter requires information on the graphite band structure and the transition matrix elements between initial and final states near the Fermi energy [19,20]. The pump-induced *changes* in the dielectric function are referenced to the unexcited sample at  $T_{e0} = 300$  K, where we use  $\hbar\omega_{\text{pl}0} = 0.9$  eV and  $\gamma_0 = 10$  THz. These values are obtained from an analysis of our measured  $\varepsilon_0(\omega)$  between 1 and 3 THz, where the Drude response dominates [17]. As seen in Fig. 1(c), for an exemplary delay of  $\tau = 0.5$  ps, the fits excellently reproduce the experimental data. In addition, the respective contributions of the IOTs and DOTs to  $\text{Im}\Delta\varepsilon_\tau$  are shown in Fig. 1(d).

In Fig. 3, the electronic temperature  $T_e$  and the Drude relaxation rate  $\gamma$  are plotted as a function of the pump-probe delay  $\tau$ , whereas changes in  $\omega_{\text{pl}}$  and  $\gamma$  are displayed versus the electronic temperature  $T_e$ . We start our discussion with the pump-induced changes  $\Delta\omega_{\text{pl}}(\tau)$  in the in-plane plasma frequency. For delays  $\tau > 0.5$  ps, it increases roughly linearly with electronic temperature. A similar rise

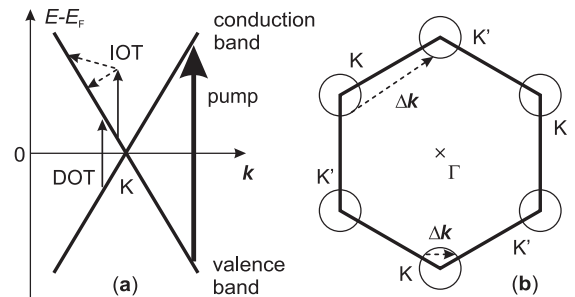


FIG. 2. (a) Sketch of the in-plane band structure of graphite close to the  $K$  or  $K'$  point where valence and conduction bands slightly overlap. Arrows indicate possible direct and indirect optical transitions induced by the probe pulse. (b) Brillouin zone perpendicular to the  $c$  axis. The Fermi surface is located around the  $K$  and  $K'$  points. Arrows mark possible scattering events of electrons and correspond to wave vector changes  $\Delta\mathbf{k}$  that are confined to the vicinity of the  $\Gamma$  and  $K$  points.

was also observed for the screened out-of-plane plasma frequency by electron energy loss spectroscopy [21]. This behavior is typical for semimetals due to their strongly varying electronic density of states near the Fermi edge and does not occur in normal metals. Figure 3(c), moreover, shows that the measured  $\Delta\omega_{\text{pl}}$  vs  $T_e$  agrees well with theoretical predictions, again based on linear response formalism and the band structure of graphite [19,20]. This agreement demonstrates the consistency of our fit results. For delays  $\tau < 0.5$  ps,  $\Delta\omega_{\text{pl}}$  vs  $T_e$  clearly leaves the linear trend. This finding indicates that the electrons have not sufficiently thermalized at this early stage after excitation, as also seen in the TRPES measurements [15].

We next consider the dynamics of the electronic temperature shown in Fig. 3(a), which contains an interesting result. With an absorbed pump fluence of  $\approx 5 \mu\text{J cm}^{-2}$  applied in our experiment and the electronic specific heat of graphite [22], the electrons in the graphite film should reach temperatures as high as  $\approx 1200$  K directly after excitation. However, as seen in Fig. 3(a), the experimentally obtained  $T_e(\tau)$  remains far below this value. We conclude that more than 90% of the absorbed pump pulse energy must have left the electronic system within the first 500 fs after excitation. Only heat transfer to the graphite lattice can explain this finding, since, in contrast to the TRPES experiment [15], ultrafast transport does not occur in our thin sample. Because of the small Fermi surface of graphite and wave vector conservation [see Fig. 2(b)], electrons are scattered solely by phonons which have the

in-plane component of their wave vector close to the  $\Gamma$  or  $K$  point of the Brillouin zone [23]. Therefore, only a quite restricted phonon subset can directly dissipate the electronic energy and heats up. These hot phonons cool down by heat transfer to cold lattice modes on a much longer time scale of  $\sim 10$  ps [24] and, thereby, dictate the observed slow decay of  $T_e$  with a time constant of 7 ps. A simple estimate [25] shows that the hot phonons occupy a fraction of  $\sim 10^{-2}$  of the Brillouin zone. Accordingly, their specific heat is that of graphite reduced by roughly the same factor. Employing these quantities [22], we estimate a maximum transient temperature increase of  $\sim 100$  K for the hot phonons, in good agreement with the experimental data in Fig. 3(a). Thus, our measurements reflect the ultrafast generation of hot phonons and their subsequent slow cooling.

Which phonon branches (acoustic or optical) dominate the initial fast cooling of the hot electrons? Recent density functional theory calculations of graphene predict an extraordinarily strong coupling between high-energy optical phonons and electrons [5]. As a consequence, these SCOP branches with quantum energies of more than 0.15 eV exhibit Kohn anomalies in their dispersion curves [4]. Since cold phonons result in a faster electron cooling than hot phonons, we first assume the SCOPs to be cold and the only lattice modes interacting with the electrons. We apply the two-temperature model [8,26] to calculate the temporal decay of  $T_e$ . With a fixed phonon temperature of 300 K and an initial electronic temperature of 380 K at  $\tau = 0.5$  ps, we obtain the dashed curve in Fig. 3(a). Since this hypothetical decay is much faster than that measured, the assumption of cold SCOPs at  $\tau = 0.5$  ps has to be wrong, and we have found further evidence for ultrafast phonon heating. In addition, other  $\Gamma$  and  $K$  phonons in graphite lead to similar decay curves only if comparable or even larger  $e$ -ph matrix elements are assumed, which is in contradiction to theoretical results [5]. To summarize, the electron cooling within only a few hundred femtoseconds is dominated by the generation of hot SCOPs. It proceeds significantly faster than in doped semiconductors [9,27] as a consequence of the strong  $e$ -ph coupling and the large phonon quantum energies. The slow decay of  $T_e$  back to 300 K provides an estimate of the SCOP lifetime of 7 ps.

While  $\partial T_e / \partial \tau$  is a measure of electronic energy relaxation, the classical Drude rate  $\gamma$  quantifies the decay of an electronic current when the driving electric field is switched off. In our experiment,  $\gamma$  shows a remarkable increase from  $\gamma_0 = 10$  THz by more than 3 THz, although  $T_e$  has increased by less than 80 K [see Fig. 3(d)]. This is in contrast to comparable measurements on  $n$ -doped InAs, where similar electronic temperatures but an order of magnitude smaller effect on  $\gamma$  were found [9]. What processes cause this significantly different behavior in graphite? For slow relaxation  $\gamma \ll \omega$  (as is the case here), the contribution to the dielectric function due to IOTs can be calculated on the basis of second-order perturbation theory resulting in a Drude-like relation [10,11]. In this formal-

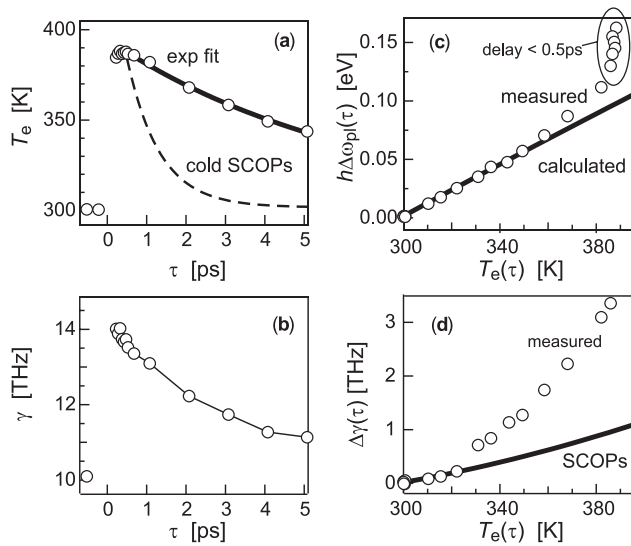


FIG. 3. (a) Temporal evolution of electronic temperature  $T_e$ . The dashed line indicates the hypothetical  $T_e$  decay if only cold SCOPs were involved; the solid line marks an exponential decay with a time constant of 7 ps. (b) Temporal evolution of the Drude relaxation rate  $\gamma$ . (c) Pump-induced change  $h\Delta\omega_{\text{pl}}$  in the unscreened plasma frequency vs electronic temperature. The solid line is a theoretical prediction. (d) Pump-induced changes  $\Delta\gamma(\tau)$  vs  $T_e(\tau)$  together with the calculated contribution due to hot SCOPs (solid line).

ism, the pump-induced changes  $\Delta\gamma$  of the current relaxation rate are caused by changes of the electronic and phononic occupation numbers. We apply this procedure to calculate the contribution of hot SCOPs to the current relaxation  $\Delta\gamma$ : The SCOP occupation numbers are assumed by Bose-Einstein distributions at temperatures that equal the respective electronic temperatures  $T_e$ . The result of this calculation is shown in Fig. 3(d). It demonstrates that hot optical phonons explain a significant part of the observed increase of the current relaxation rate [28].

We finally discuss why the measured  $\Delta\gamma$  is even larger than the calculated SCOP contribution. First, the theoretical curve should be considered as a lower limit of the true  $\Delta\gamma_{\text{SCOP}}$  since the formulas used [10,11] are expected to underestimate the current relaxation. They account only for such IOTs whose photon-related part leaves the electron in the same Bloch state. However, in graphite, resonant intermediate states in other bands can make additional contributions [10]. Furthermore, multiphonon processes are not yet accounted for in the modeled  $\Delta\gamma_{\text{SCOP}}$ . Second, electron-electron ( $e-e$ ) scattering is suggested to be quite effective in graphite due to the presence of states with both positive and negative effective mass in the Fermi surface [29,30]. This leads to the familiar relation  $\gamma_{e-e} = AT_e^2$  for the  $e-e$  scattering rate. Assuming  $\Delta\gamma_{e-e}$  to be the remaining contribution to the observed  $\Delta\gamma$ , one obtains  $A = 3.7 \times 10^7 \text{ s}^{-1} \text{ K}^{-2}$ . This value is about one order of magnitude larger than those reported for noble metals [30], which is a reasonable result:  $e-e$  interaction in graphite is much less screened than in noble metals due to the lower electron density and, unlike in free electronlike metals or doped semiconductors, no umklapp processes during  $e-e$  scattering are required to relax the electronic current. Thus, our results are consistent with strong  $e-e$  scattering as a further source of current relaxation in graphite.

In conclusion, we have investigated graphite by means of time-resolved THz spectroscopy. We find an ultrafast energy loss of optically excited electrons which is due to their strong coupling to high-energy optical phonons. Their effect was not considered in previous reports on carbon nanotubes [31]. Our work, however, underlines the importance of hot optical phonons, which also contribute significantly to the striking increase of the Drude scattering rate. Therefore, they might limit the performance of carbon nanotubes circuits not only at high electric fields [3] but also at elevated temperatures and high frequencies. We expect the electronic energy relaxation by those strongly coupled optical phonons to play an important role also in other areas such as phonon-mediated surface chemistry [32] and in laser ablation [33]. The selective excitation of only a few phonon modes may influence the desorption dynamics and products remarkably.

We thank R. Huber and A. Leitenstorfer for many helpful discussions in setting up our THz experiment, as well as F. Mauri, M. Calandra, and A. Ferrari for discussions and preprints on  $e$ -ph coupling in graphite. Generous support of the THz project by G. Ertl, the Deutsche Forschungs-

gemeinschaft, and the Schweizerischer Nationalfonds is greatly appreciated.

- 
- [1] *Graphite Fibers and Filaments*, edited by M.S. Dresselhaus *et al.* (Springer-Verlag, Berlin, 1992).
  - [2] K. S. Novoselov *et al.*, *Science* **306**, 666 (2004).
  - [3] A. Javey *et al.*, *Phys. Rev. Lett.* **92**, 106804 (2004).
  - [4] J. Maultzsch *et al.*, *Phys. Rev. Lett.* **92**, 075501 (2004).
  - [5] S. Piscanec *et al.*, *Phys. Rev. Lett.* **93**, 185503 (2004).
  - [6] R. Huber *et al.*, *Nature (London)* **414**, 286 (2001).
  - [7] R. A. Kaindl *et al.*, *Science* **287**, 470 (2000).
  - [8] P. B. Allen, *Phys. Rev. Lett.* **59**, 1460 (1987).
  - [9] T. Elsaesser *et al.*, *Phys. Rev. B* **40**, 2976 (1989).
  - [10] W. P. Dumke, *Phys. Rev.* **124**, 1813 (1961).
  - [11] P. B. Allen, *Phys. Rev. B* **3**, 305 (1971); R. von Baltz and W. Escher, *Phys. Status Solidi B* **51**, 499 (1972).
  - [12] R. Huber *et al.*, *Appl. Phys. Lett.* **76**, 3191 (2000).
  - [13] Q. Wu and X. C. Zhang, *Appl. Phys. Lett.* **71**, 1285 (1997).
  - [14] We Fourier-transform the data with respect to  $t$  and use standard Fresnel formulas to obtain the dielectric function. For details, see R. D. Averitt *et al.*, *J. Phys. Condens. Matter* **14**, R1357 (2002).
  - [15] G. Moos *et al.*, *Phys. Rev. Lett.* **87**, 267402 (2001).
  - [16] K. Seibert *et al.*, *Phys. Rev. B* **42**, 2842 (1990).
  - [17] H. R. Philipp, *Phys. Rev. B* **16**, 2896 (1977).
  - [18] H. Ehrenreich and M. H. Cohen, *Phys. Rev.* **115**, 786 (1959); S. L. Adler, *Phys. Rev.* **126**, 413 (1962).
  - [19] K. Nakao, *J. Phys. Soc. Jpn.* **47**, 208 (1979).
  - [20] We obtain the band structure and transition matrix elements required by numerically diagonalizing the  $4 \times 4$  Hamiltonian of the Slonczewski-Weiss-McClure model. This semiphenomenological model well describes the electronic  $\pi$  bands of graphite around  $E_F$  [1].
  - [21] E. T. Jensen *et al.*, *Phys. Rev. Lett.* **66**, 492 (1991).
  - [22] T. Nihira and T. Iwata, *Phys. Rev. B* **68**, 134305 (2003).
  - [23] R. Saito *et al.*, *Phys. Rev. Lett.* **88**, 027401 (2002).
  - [24] T. Mishina *et al.*, *Phys. Rev. B* **62**, 2908 (2000).
  - [25] Figure 2(b) shows that electrons of higher energy  $E-E_F$  will emit or absorb phonons out of a larger wave vector range. Assuming  $E-E_F$  to be at most half the pump photon energy, the electron band slope implies that only  $\sim 10^{-2}$  of all phonon wave vectors directly interact with the electrons.
  - [26] We start with Eq. (6) from Ref. [8] and use the  $e$ -ph matrix elements and their directional dependence from Ref. [5].
  - [27] H. P. M. Pellemans and P. C. M. Planken, *Phys. Rev. B* **57**, R4222 (1998).
  - [28] Substantial contributions to  $\Delta\gamma$  by other phonons near  $\Gamma$  and  $K$ , acoustic phonons, or lattice defects are largely negligible, since they are only weakly coupled to the electronic system [5].
  - [29] P. F. Maldague and C. A. Kukkonen, *Phys. Rev. B* **19**, 6172 (1979).
  - [30] M. Kaveh and N. Wisser, *Adv. Phys.* **33**, 257 (1984).
  - [31] T. Hertel and G. Moos, *Phys. Rev. Lett.* **84**, 5002 (2000); M. Zamkov *et al.*, *Phys. Rev. Lett.* **94**, 056803 (2005).
  - [32] M. Bonn *et al.*, *Science* **285**, 1042 (1999).
  - [33] H. O. Jeschke *et al.*, *Phys. Rev. Lett.* **87**, 015003 (2001).